Zentrum für Technomathematik

Fachbereich 3 – Mathematik und Informatik

Reconstruction of Reflectivity Desities by Wavelet Transforms

Stephan Dahlke **Peter Maaß**
Gerd Teschke

Report 01–10

Berichte aus der Technomathematik

Report 01–10 **August 2001**

Reconstruction of Reflectivity Densities by Wavelet Transforms

Stephan Dahlke*, Peter Maass †, Gerd Teschke ‡
Fachbereich 3
Universität Bremen
Postfach 33 04 40
28334 Bremen
Germany

Abstract

This paper is concerned with reconstruction problems arising in the context of radar signal analysis. The goal in radar is to obtain information about objects by emitting certain signals and analyzing the reflected echoes. In this paper, we shall focus on the general wideband model for radar echoes and on the case of continuously distributed objects D (reflectivity density).

In this case, the echo is given by an inverse wavelet transform of the density D where the role of the analyzing wavelet is played by the transmitted signal. However, the null space of an inverse wavelet transform is non trivial, it is described by the corresponding reproducing kernel. Following the approach of H. Naparst [13] and L. Rebolla et al. [15] we suggest to treat this problem by transmitting not just one signal but a family of signals. Indeed, a reconstruction formula for one and two dimensional reflectivity densities can be derived, provided that the set of outgoing signals forms an orthogonal basis or – more general – a frame. We also present some rigorous error estimates for these reconstruction formulas. The theoretical results are confirmed by some numerical examples. We also briefly discuss the generalization of our approach to the narrowband regime.

Key Words: Radar, reflectivity density, wideband regime, narrowband regime, frames, wavelets, generalized Sobolev spaces.

AMS Subject classification: 41A25, 42C15, 42C40, 65J22

*The work of this author has been partially supported by Deutsche Forschungsgemeinschaft, Grants Da 117/13–1, Da 360/4–1.

†The work of this author has been partially supported by Deutsche Forschungsgemeinschaft, Grant Ma 1657/6–1.

‡The work of this author has been partially supported by BMBF, Grant 3MAM1HB.

1 Introduction

In recent years, wavelet analysis has been successfully applied to many problems in signal analysis and image processing as well as to applications in numerical analysis. Moreover, since the pioneering work of Naparst [13, 14], it is well–known that the specific features of wavelets can also be used efficiently for treating reconstruction problems in the context of radar signal analysis. Related approaches for radar applications have been investigated by [11, 12], more recently the original approach of Naparst has been extended by [15].

The basic radar problem asks to gain information about an object by analyzing waves reflected from it. To describe this simplified setting, let us first assume that the object under consideration can be described as a point, moving with constant velocity v towards or away from a given source. The distance between object and source at time $t = 0$ is denoted be R. The emitted signal is denoted by $h(t)$, then the *wideband model* for the received echo $f(t)$ is given by

$$f(t) \;=\; \sqrt{|s|}\; h(s(t-\tau)), \tag{1.1}$$

where the *Doppler scale factor* s is obtained from the speed of light c and the object velocity v as

$$s = \frac{c-v}{c+v}, \tag{1.2}$$

and the delay τ is determined by the distance R between the object and the source as

$$\tau = \frac{2R}{c-v}. \tag{1.3}$$

The so-called Doppler coordinates (s, τ) are in one–to–one correspondence to the desired values v and R. The multiplicative factor $\sqrt{|s|}$ is chosen such that the energy is conserved, i.e., we assume a perfectly reflecting object. For further information, the reader is referred, e.g., to [7, 8, 9].

In the presence of many objects the total echo is modeled as the superposition of the single echoes. More general, if we assume that we want to observe a reflecting continuum with varying reflectivity as described in Doppler coordinates by a *reflectivity density* $D(\tau, 1/s)$, then the total echo is given by

$$f(t) = \int_{\mathbf{R}} \int_{\mathbf{R}\setminus\{0\}} D(\tau, s)|s|^{-1/2} h\left(\frac{t-\tau}{s}\right) \frac{ds d\tau}{s^2}. \tag{1.4}$$

Consequently, the task is to reconstruct the density $D(\tau, s)$ from the received echo. To treat this problem, let us first remark that formula (1.4) can be reinterpreted in the context of wavelet analysis: In general, the *continuous wavelet transform* $W_\psi(F)$ of a function $F \in L_2(\mathbf{R})$ is given by

$$(W_\psi F)(a, b) := \int_{\mathbf{R}} F(x)\; |a|^{-1/2} \overline{\psi\left(\frac{x-b}{a}\right)} dx. \tag{1.5}$$

This transformation is well–defined, provided that the analyzing wavelet ψ satisfies the admissibility condition

$$C_\psi \;=\; \int_{\mathbf{R}} \frac{|\hat{\psi}(\xi)|^2}{|\xi|} d\xi < \infty. \tag{1.6}$$

The wavelet transform W_ψ is a multiple of an isometry whose inverse is given by the adjoint wavelet transform

$$F(x) = W_\psi^* \left(W_\psi F(a,b)\right)(x) = \frac{1}{C_\psi} \int_{\mathbf{R}} \int_{\mathbf{R}\setminus\{0\}} (W_\psi F)(a,b)\ |a|^{-1/2} \psi\left(\frac{x-b}{a}\right) \frac{da}{a^2} db, \tag{1.7}$$

see, e.g., [3, 7, 10] for details. Therefore a comparison of (1.7) with (1.4) yields the well-known and basic identity which links wideband radar echoes to wavelet analysis, see e.g. [13, 12]: the echo f is identical with the inverse wavelet transform of the searched reflectivity distribution D where the transmitted signal h plays the role of the analyzing wavelet.

This suggests to recover D by computing the wavelet transform of the echo f:

$$D(\tau, s) := \frac{1}{C_h}[(W_h f)(\tau, s)]. \tag{1.8}$$

However, the null space $\mathcal{N}$ of an inverse wavelet transform is non trivial. Hence by this procedure one can only recover the component of D which lies in the orthogonal complement of $\mathcal{N}$ or equivalently one can recover the component of D in the range of the wavelet transform W_h.

To our knowledge, there exists no physical principle that guarantees that D is in fact contained in the range of W_h, so that (1.8) only describes one part of the desired density D. Inspired by these problems, Naparst [13, 14] was the first one who suggested not to transmit just *one* signal but a *family* of signals. In his fundamental work, Naparst primarily studied the case that the transmitted signals form an orthonormal basis. However, this assumption is very restrictive in practice. Therefore, quite recently, Rebollo–Neira, Platino and Fernandez–Rubio generalized Naparst's approach to the case of transmitting a *frame* of signals, which is a much weaker restriction, [15]. The present study is very much inspired by their results, however, we modify and generalize their approach in the following sense:

- rigorous error estimates in suitably weighted Sobolev spaces are given in Section 3;
- a generalization to the multivariate case is discussed in Section 4, this includes an inversion formula for a suitable subclass of 2D reflectivity distributions;
- numerical examples using orthogonal and biorthogonal wavelets confirm the theoretical results in Section 5;
- an investigation of the *narrowband model* is contained in Section 6.

Moreover, the proof of the basic reconstruction formula in Section 2 is significantly shorter compared to the exposition in [15].

2 Basic Reconstruction Formulas

In general, the reflectivity distribution $D(\tau, s)$ cannot be reconstructed from the knowledge of a single echo. Following the approach of [13, 15] we assume that echoes

$$f_m(t) = \int_{\mathbf{R}} \int_{\mathbf{R}\setminus\{0\}} D(\tau, s)|s|^{-1/2} h_m\left(\frac{t-\tau}{s}\right) \frac{ds d\tau}{s^2}. \tag{2.1}$$

are available for a family of submitted signals $\{h_m\}_{m\in\mathbf{Z}}$. H. Naparst proved a reconstruction formula under the assumption that $\{h_m\}_{m\in\mathbf{Z}}$ forms an orthogonal basis. We follow the approach of Rebolla et al. and assume a weaker condition, namely that $\{h_m\}_{m\in\mathbf{Z}}$ forms a frame in $L_2(\mathbf{R})$. The original proof in [15] is somewhat complicated and long, we will present a shorter proof using some standard Fourier techniques.

Let us briefly recall the notion of a frame. In general, a system $\{h_m\}_{m\in\mathbf{Z}}$ of functions is called a *frame* if there exist constants A and B, $0 < A \leq B < \infty$, such that

$$A\|F\|^2_{L_2(\mathbf{R})} \leq \sum_{m\in\mathbf{Z}} |\langle F, h_m\rangle|^2 \leq B\|F\|^2_{L_2(\mathbf{R})}. \tag{2.2}$$

The numbers A, B are called *frame bounds*. Given a frame $\{h_m\}_{m\in\mathbf{Z}}$, one defines the *frame operator* T as

$$T(F) := \sum_{m\in\mathbf{Z}} \langle F, h_m\rangle h_m. \tag{2.3}$$

For later use, let us recall the following fundamental theorem which was proved in [5].

Theorem 2.1 *Let $\{h_m\}_{m\in\mathbf{Z}}$ be a frame in $L_2(\mathbf{R})$. Then the following holds.*

i) T is invertible and $B^{-1}I \leq T^{-1} \leq A^{-1}I$.

ii) $\{h^m\}_{m\in\mathbf{Z}}$, $h^m := T^{-1}h_m$ is a frame with bounds A^{-1}, B^{-1}, called the dual frame *of $\{h_m\}_{m\in\mathbf{Z}}$.*

iii) Every $F \in L_2(\mathbf{R})$ can be written as

$$F = \sum_{m\in\mathbf{Z}} \langle F, h^m\rangle h_m = \sum_{m\in\mathbf{Z}} \langle F, h_m\rangle h^m. \tag{2.4}$$

Furthermore we need a result concerning the Fourier transform of frames.

Lemma 2.1 *Let $\{h_m\}_{m\in\mathbf{Z}}$ be a frame and let $\{h^m\}_{m\in\mathbf{Z}}$ denote the dual frame. Then the set $\{\hat{h}_m\}_{m\in\mathbf{Z}}$ also constitutes a frame and the dual frame is defined by $(\hat{h})^m = \frac{1}{(2\pi)}\widehat{h^m}$.*

Proof: First of all, we show that the set $\{\hat{h}_m\}_{m\in\mathbf{Z}}$ with

$$\hat{h}_m(\omega) = \int_{I\!R} h_m(x) e^{-i\omega x}\, dx \tag{2.5}$$

is a frame. By Plancherel's Theorem, we obtain

$$\begin{aligned} A\|f\|^2_{L_2(\mathbf{R})} &= (2\pi)\ A\ \|\check{f}\|^2_{L_2(\mathbf{R})} \leq (2\pi) \sum_{m\in\mathbf{Z}} |\langle \check{f}, h_m\rangle|^2 \\ &= \sum_{m\in\mathbf{Z}} |\langle f, \hat{h}_m\rangle|^2 \leq (2\pi) B\|\check{f}\|^2_{L_2(\mathbf{R})} = B\|f\|^2_{L_2(\mathbf{R})}. \end{aligned} \tag{2.6}$$

It remains to identify the reciprocal frame. The decomposition

$$f = \sum_{m\in\mathbf{Z}} \langle h_m, f\rangle h^m$$

implies

$$\hat{f} = \sum_{m\in\mathbf{Z}} \langle h_m, f\rangle \widehat{h^m} = \frac{1}{(2\pi)} \sum_{m\in\mathbf{Z}} \langle \hat{h}_m, \hat{f}\rangle \widehat{h^m},$$

and the result follows by another application of Plancherel's Theorem. □

Using the frame theoretic approach, the following reconstruction formula holds.

Theorem 2.2 *Let $\{h_m\}_{m\in\mathbf{Z}}$ be a frame of outgoing signals in $L_2(\mathbf{R})$ and let f_m denote the corresponding echoes produced by a reflectivity density $D(\tau, s)$,*

$$f_m(t) = \int_{\mathbf{R}} \int_{\mathbf{R}\setminus\{0\}} D(\tau, s)|s|^{-1/2} h_m\left(\frac{t-\tau}{s}\right) \frac{ds d\tau}{s^2}. \tag{2.7}$$

Let us assume that the following conditions are satisfied

$$D(\tau, s)|s|^{-1/2} h_m\left(\frac{t-\tau}{s}\right) \in L_1(\frac{ds dt d\tau}{s^2}),\ \widehat{D(\cdot, s)}(\omega) \in L_1(d\omega),\ \widehat{D(\cdot, \sigma)}(\omega)|\sigma|^{-3/2} \in L_2(d\sigma). \tag{2.8}$$

Then $D(\tau, s)$ can be reconstructed as follows

$$\begin{aligned} D(\tau, s) &= \frac{1}{(2\pi)^2} \sum_{m\in\mathbf{Z}} \int_{-\infty}^{0} -\frac{1}{i} \widehat{f'_m}(\omega) \widehat{h^m(\frac{\cdot}{s})}(\omega)|s|^{1/2} e^{i\tau\omega} d\omega \\ &\quad + \frac{1}{(2\pi)^2} \sum_{m\in\mathbf{Z}} \int_{0}^{\infty} \frac{1}{i} \widehat{f'_m}(\omega) \widehat{h^m(\frac{\cdot}{s})}(\omega)|s|^{1/2} e^{i\tau\omega} d\omega, \end{aligned} \tag{2.9}$$

where $\{h^m\}_{m\in\mathbf{Z}}$ denotes the reciprocal frame of $\{h_m\}_{m\in\mathbf{Z}}$.

Proof: We first observe that

$$|s|^{-1/2} h_m\left(\widehat{\frac{\cdot-\tau}{s}}\right)(\omega) = |s|^{1/2} e^{-i\omega\tau} \hat{h}_m(\omega s). \tag{2.10}$$

Therefore, applying Fourier transforms to (2.7) and interchanging the order of integration yields

$$\begin{aligned} \hat{f}_m(\omega) &= \int_{\mathbf{R}} \int_{\mathbf{R}\setminus\{0\}} D(\tau, s) \int_{\mathbf{R}} |s|^{-1/2} h_m\left(\frac{t-\tau}{s}\right) e^{-i\omega t} dt \frac{ds d\tau}{s^2} \\ &= \int_{\mathbf{R}} \int_{\mathbf{R}\setminus\{0\}} D(\tau, s)|s|^{1/2} e^{-i\omega\tau} \hat{h}_m(s\omega) \frac{ds d\tau}{s^2} \\ &= \int_{\mathbf{R}\setminus\{0\}} \widehat{D(\cdot, s)}(\omega) \hat{h}_m(s\omega)|s|^{-3/2} ds. \end{aligned}$$

Observe that all modifications performed above are justified by (2.8). Hence, by employing the substitution $\sigma = s\omega$, we obtain

$$\begin{aligned}
\hat{f}_m(\omega) &= \int_{\mathbf{R}\setminus\{0\}} \widehat{D(\cdot, \frac{\sigma}{\omega})}(\omega)\hat{h}_m(\sigma)|\frac{\sigma}{\omega}|^{-3/2}|\omega|^{-1}d\sigma \\
&= \int_{\mathbf{R}\setminus\{0\}} \widetilde{D}(\omega,\sigma)\hat{h}_m(\sigma)d\sigma \\
&= \langle \widetilde{D}(\omega,\cdot), \hat{h}_m(\cdot)\rangle, \qquad (2.11)
\end{aligned}$$

where $\widetilde{D}(\omega,\sigma)$ is defined by

$$\widetilde{D}(\omega,\sigma) := \widehat{D(\cdot, \frac{\sigma}{\omega})}(\omega)|\omega|^{1/2}|\sigma|^{-3/2}. \qquad (2.12)$$

From (2.11), we observe that the quantities $\hat{f}_m(\omega)$ can be interpreted as the coefficients of $\widetilde{D}(\omega,\cdot)$ with respect to the set $\{\hat{h}_m\}_{m\in\mathbf{Z}}$. However, from Lemma 2.1 we know that this set also constitutes a frame with reciprocal frame $(\hat{h})^m = \frac{1}{(2\pi)}\widehat{h^m}$. Therefore, by using the identity

$$f = \frac{1}{(2\pi)}\sum_{m\in\mathbf{Z}} \langle f, \hat{h}_m\rangle \widehat{h^m}, \qquad (2.13)$$

we may reconstruct $\widetilde{D}(\omega,\sigma)$ as

$$\begin{aligned}
\widetilde{D}(\omega,\sigma) &= \frac{1}{(2\pi)}\sum_{m\in\mathbf{Z}} \langle \widetilde{D}(\omega,\cdot), \hat{h}_m(\cdot)\rangle \widehat{h^m}(\sigma) \\
&= \frac{1}{(2\pi)}\sum_{m\in\mathbf{Z}} \hat{f}_m(\omega)\widehat{h^m}(\sigma). \qquad (2.14)
\end{aligned}$$

From (2.14), we can now also reconstruct the density $D(\tau,s)$. By using the definition (2.12) we obtain

$$\widehat{D(\cdot, \frac{\sigma}{\omega})}(\omega) = \frac{1}{(2\pi)}\sum_{m\in\mathbf{Z}} \hat{f}_m(\omega)\widehat{h^m}(\sigma)|\sigma|^{3/2}|\omega|^{-1/2}$$

which yields

$$\begin{aligned}
\widehat{D(\cdot, s)}(\omega) &= \frac{1}{(2\pi)}\sum_{m\in\mathbf{Z}} \hat{f}_m(\omega)\widehat{h^m}(\omega s)|\omega||s|^{3/2} \\
&= \frac{1}{(2\pi)}\sum_{m\in\mathbf{Z}} \hat{f}_m(\omega)|\omega|\widehat{h^m(\frac{\cdot}{s})}(\omega)|s|^{1/2}. \qquad (2.15)
\end{aligned}$$

Now the result follows by applying the one–dimensional inverse Fourier transform to both sides of (2.15)

$$D(\tau,s) = \frac{1}{(2\pi)}\int_{\mathbf{R}} \widehat{D(\cdot,s)}(\omega)e^{i\tau\omega}d\omega$$

$$
\begin{aligned}
&= \frac{1}{(2\pi)^2}\sum_{m\in\mathbf{Z}}\int_{\mathbf{R}}\hat{f}_m(\omega)|\omega|\widehat{h^m(\frac{\cdot}{s})}(\omega)|s|^{1/2}e^{i\tau\omega}d\omega\\
&= \frac{1}{(2\pi)^2}\sum_{m\in\mathbf{Z}}\int_{-\infty}^{0}-\omega\hat{f}_m(\omega)\widehat{h^m(\frac{\cdot}{s})}(\omega)|s|^{1/2}e^{i\tau\omega}d\omega\\
&\quad+\frac{1}{(2\pi)^2}\sum_{m\in\mathbf{Z}}\int_{0}^{\infty}\omega\hat{f}_m(\omega)\widehat{h^m(\frac{\cdot}{s})}(\omega)|s|^{1/2}e^{i\tau\omega}d\omega\\
&= \frac{1}{(2\pi)^2}\sum_{m\in\mathbf{Z}}\int_{-\infty}^{0}-\frac{1}{i}\widehat{f'_m}(\omega)\widehat{h^m(\frac{\cdot}{s})}(\omega)|s|^{1/2}e^{i\tau\omega}d\omega\\
&\quad+\frac{1}{(2\pi)^2}\sum_{m\in\mathbf{Z}}\int_{0}^{\infty}\frac{1}{i}\widehat{f'_m}(\omega)\widehat{h^m(\frac{\cdot}{s})}|s|^{1/2}e^{i\tau\omega}d\omega.
\end{aligned}
$$

□

We would like to conclude this section on reconstruction formulae for wideband radar models with a reference to an elegant but rather different approach. Assume that the signal $h_m(t) \sim \delta(t - t_m)$ is a short pulse at time t_m. Then, the echo (1.4) at time t is equivalent to the integration of D along the line $\tau = t - st_m$. I.e. the echoes resemble the Radon transform of D, they can then be inverted by tomographic inversion procedures, see [6].

3 Error Estimates

In the previous section, we have derived a method to reconstruct the reflectivity density from the observed echoes. However, the applicability of this method to real–life problems is diminished by the fact that the underlying frame usually contains *infinitely* many elements. Clearly, in practice, only a finite number of frame elements can be transmitted. Hence we are faced with the problem of choosing appropriate collections. Furthermore, it is clearly desirable to have some information concerning the resulting approximation properties for different choices of frames.

The derivation of the error bounds rests on a Jackson type estimate for the frame $\{\hat{h}_m\}_{m\in\mathbf{Z}}$. Let us assume that this set of functions allows an ordering by index sets $I_J \subset \mathbf{Z}$, s.t. an Jackson type estimate of the form

$$
\|g - \sum_{m\in I_J}\langle g, \hat{h}_m\rangle \hat{h^m}\|_{L_2(\mathbf{R})} \;\lesssim\; 2^{-2J\alpha}\;|g|^2_{H^\alpha(\mathbf{R})}
$$

holds. (In the sequel, ' $\lesssim$ ' will always indicate inequality up to constant factors). H^α denotes the Sobolev space of order α, see e.g. [1].

Such estimates are known for a variety of functions, e.g. trigonometric polynomials and hierarchical finite elements. In the context of wavelet analysis, this requirement is met by orthogonal or biorthogonal wavelets. Let us therefore assume that the frame $\{h_m\}_{m\in\mathbf{Z}}$ consists of the inverse Fourier transforms of the elements of an orthonormal wavelet basis, i.e.,

$$
h_m = h_{m(j,k)} = \mathcal{F}^{-1}\psi_{j,k}, \quad \psi_{j,k}(x) = 2^{j/2}\psi(2^j x - k), \quad j,k \in \mathbf{Z}, \tag{3.1}
$$

where the functions $\psi_{j,k}$ satisfy

$$\langle \psi_{j,k}, \psi_{j',k'} \rangle = \delta_{j,j'} \delta_{k,k'}. \tag{3.2}$$

We may e.g. use the compactly supported wavelet basis constructed by Daubechies [3]. Then we do not employ all functions in the resulting frame, but only those up to a given refinement level J. For this specific setting, the following result in the weighted L_2–space $L_2(\mathbf{R}^2, d\tau \frac{ds}{|s|^3})$ holds.

Theorem 3.1 *Let $N-1$ denote the degree of polynomial exactness of the multiresolution analysis $\{V_j\}_{j \in \mathbf{Z}}$ associated with the wavelet ψ. Suppose that for some fixed $\alpha < N$ the condition*

$$G(\alpha, \omega) := |\widetilde{D}(\omega, \cdot)|^2_{H^\alpha(\mathbf{R})} < \infty \tag{3.3}$$

is satisfied. Then, the following error estimate holds:

$$\int_{\mathbf{R}} \int_{\mathbf{R}} \left| D(\tau, s) - \frac{1}{(2\pi)^2} \sum_{j \le J} \int_{\mathbf{R}} \hat{f}_m(\omega) \hat{h}_m(s\omega) |\omega| |s|^{3/2} e^{i\tau\omega} d\omega \right|^2 d\tau \frac{ds}{|s|^3} \lesssim 2^{-2J\alpha} \int_{\mathbf{R}} |\omega| G(\alpha, \omega) d\omega. \tag{3.4}$$

If α is an integer, the function $G(\alpha, \omega)$ can be estimated in terms of the density D as follows:

$$G(\alpha, \omega) \lesssim \sum_{\beta \le \alpha} |\omega|^{1+2\beta-2\alpha} \int_{\mathbf{R}} |\widehat{(\frac{\partial}{\partial \sigma}^{\alpha-\beta} D)}(\cdot, \frac{\sigma}{\omega})(\omega) \sigma^{3/2-\beta}|^2 d\sigma. \tag{3.5}$$

Proof: Classical wavelet analysis provides us with the following Jackson-type estimate:

$$\| \widetilde{D}(\omega, \cdot) - \frac{1}{(2\pi)} \sum_{j \le J} \hat{f}_m(\omega) \hat{h}_m(\cdot) \|^2_{L_2(\mathbf{R})} \lesssim 2^{-2J\alpha} |\widetilde{D}(\omega, \cdot)|^2_{H^\alpha(\mathbf{R})}, \tag{3.6}$$

see, e.g., [4] for details. Hence, by using (2.12) and substituting $\sigma = s\omega$ we obtain

$$\begin{aligned} 2^{-2J\alpha} G(\alpha, \omega) &\gtrsim \| \widehat{D(\cdot, \frac{\sigma}{\omega})}(\omega) |\omega|^{1/2} |\sigma|^{-3/2} - \frac{1}{(2\pi)} \sum_{j \le J} \hat{f}_m(\omega) \hat{h}_m(\sigma) \|_{L_2(d\sigma)} \\ &= \int_{\mathbf{R}} \left| \widehat{D(\cdot, s)}(\omega) - \frac{1}{(2\pi)} \sum_{j \le J} \hat{f}_m(\omega) \hat{h}_m(s\omega) |\omega| |s|^{3/2} \right|^2 |\omega| |\omega|^{-2} \frac{ds}{|s|^3} \end{aligned} \tag{3.7}$$

Therefore multiplying both sides of (3.7) by $|\omega|$, integrating with respect to ω and applying Plancherel's Theorem for another time yields

$$\begin{aligned} 2^{-2J\alpha} \int_{\mathbf{R}} |\omega| G(\alpha, \omega) d\omega &\gtrsim \int_{\mathbf{R}} \int_{\mathbf{R}} \left| \widehat{D(\cdot, s)}(\omega) - \sum_{j \le J} \hat{f}_m(\omega) \hat{h}_m(s\omega) |\omega| |s|^{3/2} \right|^2 d\omega \frac{ds}{|s|^3} \\ &= (2\pi) \int_{\mathbf{R}} \int_{\mathbf{R}} \left| D(\tau, s) - \frac{1}{(2\pi)^2} \sum_{j \le J} \int_{\mathbf{R}} \hat{f}_m(\omega) \hat{h}_m(s\omega) |\omega| |s|^{3/2} e^{i\tau\omega} d\omega \right|^2 d\tau \frac{ds}{|s|^3}. \end{aligned} \tag{3.8}$$

It remains to establish (3.5). By using Leibnitz' rule we obtain

$$
\begin{aligned}
|\widetilde{D}(\omega,\cdot)|^2_{H^\alpha(\mathbf{R})} &= \int_{\mathbf{R}} \left| \frac{\partial}{\partial\sigma}^{\alpha} (\widetilde{D}(\omega,\cdot)) \right|^2 d\sigma \\
&= \int_{\mathbf{R}} \left| \frac{\partial}{\partial\sigma}^{\alpha} (\widehat{D(\cdot,\frac{\sigma}{\omega})}(\omega)|\omega|^{1/2}|\sigma|^{-3/2}) \right|^2 d\sigma \\
&= |\omega| \int_{\mathbf{R}} \left| \frac{\partial}{\partial\sigma}^{\alpha} (\int_{\mathbf{R}} D(\tau,\frac{\sigma}{\omega}) e^{-i\omega\tau} d\tau \sigma^{-3/2}) \right|^2 d\sigma \\
&= |\omega| \int_{\mathbf{R}} \left| \sum_{\beta\le\alpha} \binom{\alpha}{\beta} \frac{\partial}{\partial\sigma}^{\alpha-\beta} (\int_{\mathbf{R}} D(\tau,\frac{\sigma}{\omega}) e^{-i\omega\tau} d\tau) (\frac{\partial}{\partial\sigma}^{\beta} \sigma^{-3/2}) \right|^2 d\sigma \\
&= |\omega| \int_{\mathbf{R}} | \sum_{\beta\le\alpha} \binom{\alpha}{\beta} (\int_{\mathbf{R}} (\frac{\partial}{\partial\sigma}^{\alpha-\beta} D)(\tau,\frac{\sigma}{\omega}) \omega^{\beta-\alpha} e^{-i\omega\tau} d\tau) \\
&\qquad \cdot (-\frac{3}{2})(-\frac{3}{2}-1)\dots(-\frac{3}{2}-\beta-1)\sigma^{-3/2-\beta}|^2 d\sigma \\
&= |\omega| \int_{\mathbf{R}} | \sum_{\beta\le\alpha} \binom{\alpha}{\beta} (\widehat{\frac{\partial}{\partial\sigma}^{\alpha-\beta} D})(\cdot,\frac{\sigma}{\omega})(\omega) \omega^{\beta-\alpha} \prod_{l=0}^{\beta-1} (-\frac{3}{2}-l)\sigma^{-3/2-\beta}|^2 d\sigma \\
&\lesssim \sum_{\beta\le\alpha} |\omega|^{1+2\beta-2\alpha} \int_{\mathbf{R}} |(\widehat{\frac{\partial}{\partial\sigma}^{\alpha-\beta} D})(\cdot,\frac{\sigma}{\omega})(\omega)\sigma^{-3/2-\beta}|^2 d\sigma,
\end{aligned}
$$

and (3.5) is shown. □

4 The Multivariate Case

In this section, we want to investigate to what extent the analysis presented above can be generalized to the multivariate case. In the sequel, we shall especially focus on the 2D-case. First of all, we have to derive a suitable mathematical model which describes the echoes produced by a two-dimensional reflectivity distribution. Secondly, we have to analyze how this reflectivity density can be reconstructed from these echoes.

4.1 A 2D-Model

For univariate signals in $L_2(\mathbf{R})$, the model (1.4) which describes the echoes produced by a reflectivity density is well–established. This model deals with signals which are modulated over time, i.e., the signal is a function $h(t)$. However, this only allows to reconstruct the velocities in the direction of the emitted beam, i.e., only the radial component of the velocity field can be analyzed.

It seems that much less is known for the higher dimensional cases. In general one might assume, that the signal is emitted in a three dimensional cone. In principle, one might then emit signals, which are modulated differently for each beam in this cone, i.e., the emitted signal is a function $h(t,\gamma,\zeta)$, where γ and ζ are the angles of the cone.

In this paper, we want to treat a two dimensional model as a first step. Here we assume, that the signal is emitted as a fan. Moreover, we assume that the positions of the reflecting entities, as described by the support of the reflectivity distribution D, are sufficiently far away, so that we can treat the fan of beams as a set of parallel beams instead. Let us assume, that the beams are aligned on the x-axis, i.e., the emitted signal is modelled by a function $h(t,x)$, and that the signal is emitted in the direction of the y-axis.

We follow the approach of Section 1 in order to model mathematically the resulting echoes. Hence let us first consider the case of a single point object, which is moving in the (x,y)–plane. We further assume that the measurement process lives on a shorter time scale compared to the velocity of the object. Hence, we can neglect any acceleration of the object and we simply assume that the trajectory of the object is given by

$$(x(t), y(t)) = (x_0 + tv_x, y_0 + tv_y). \tag{4.1}$$

Again, we introduce Doppler variables

$$s_0 := \frac{c+v_y}{c-v_y}, \qquad \tau_0 := \frac{2y_0}{c-v_y}. \tag{4.2}$$

At time t the moving object is at a position with y-coordinate $y_0 + tv_y$, i.e., at this instant it reflects a signal which was send out at time $t - \frac{y_0+tv_y}{c}$ at the corresponding position $x_0 + tv_x$. Altogether, the object reflects the signal

$$s(t) = h(t - \frac{y_0 + tv_y}{c}, x_0 + tv_x) \ .$$

This signal then produces an echo at position $x = x_0 + tv_x$ which is time delayed by $\frac{y_0+tv_y}{c}$, i.e., this yields an echo

$$e(t + \frac{y_0 + tv_y}{c}, x_0 + tv_x) = s(t) = h(t - \frac{y_0 + tv_y}{c}, x_0 + tv_x) \quad . \tag{4.3}$$

We define the auxiliary parameters

$$\sigma_0 := v_x \frac{1+s_0}{2s_0}, \qquad \text{and} \quad z_0 = x_0 - \frac{v_x \tau_0}{2s_0}. \tag{4.4}$$

Lemma 4.1 *Suppose that the object is moving with velocity $v = (v_x, v_y)$ in the (x,y)–plane and that a signal $h(x,t)$ is transmitted. Then the echo produced by the object is given by*

$$e(t, z_0 + t\sigma_0) = h(\frac{t-\tau_0}{s_0}, z_0 + t\sigma_0) \ . \tag{4.5}$$

Proof:
We start with equation (4.3) and use the substitution $t \to t + \frac{y_0+tv_y}{c}$, which yields

$$e(t, x_0 + \left(\frac{ct - y_0}{c+v_y}\right) v_x) = h(\left(\frac{ct-y_0}{c+v_y}\right) \frac{c-v_y}{c} - \frac{y_0}{c}, x_0 + \left(\frac{ct-y_0}{c+v_y}\right) v_x) \quad .$$

Rewriting this equation in Doppler coordinates and using the auxiliary parameters (4.4) yields

$$e(t, z_0 + t\sigma_0) = h(\frac{t - \tau_0}{s_0}, z_0 + t\sigma_0) \ . \tag{4.6}$$

and the lemma is proved. □

The set of parameters $(\tau_0, s_0, z_0, \sigma_0)$ is in one–to–one correspondence to the original variables (x_0, v_x, y_0, v_y). Hence, similar to the 1D–case, we describe a dense target environment by a reflectivity distribution $D(\tau_0, s_0, z_0, \sigma_0)$. Note, that we use a slightly different notation for the Doppler coordinates in the 2D–case: the variable s in the 1D–model corresponds to the variable $1/s_0$ in the 2D–case. This avoids the term ds/s^2, moreover, we have neglected the scaling term $\sqrt{s}$. We now obtain the following model for describing the 2D–echo.

Corollary 4.1 *The echo produced by a reflectivity density $D(\tau_0, s_0, z_0, \sigma_0)$ is given by*

$$e(t,x) = \int_{\mathbf{R}}\int_{\mathbf{R}}\int_{\mathbf{R}}\int_{\mathbf{R}} D(\tau_0, s_0, z_0, \sigma_0)\delta(x - (z_0 + \sigma_0 t))h\left(\frac{t - \tau_0}{s_0}, z_0 + \sigma_0 t\right) d\tau_0 ds_0 d\sigma_0 dz_0. \tag{4.7}$$

Proof:
We rewrite the echo of a single object as

$$e(t,x) := \delta(x - (z_0 + \sigma_0 t))h(\frac{t - \tau_0}{s_0}, z_0 + \sigma_0 t). \tag{4.8}$$

Consequently, for the case of a nontrivial reflectivity density, we obtain

$$e(t,x) = \int_{\mathbf{R}}\int_{\mathbf{R}}\int_{\mathbf{R}}\int_{\mathbf{R}} D(\tau_0, s_0, z_0, \sigma_0)\delta(x - (z_0 + \sigma_0 t))h(\frac{t - \tau_0}{s_0}, z_0 + \sigma_0 t) d\tau_0 ds_0 d\sigma_0 dz_0.$$

proving the corollary. □

4.2 The Reconstruction Problem

Once the model described in Corollary 4.1 is given, it is natural to ask for a suitable reconstruction formula to extract the unknown density D. Again we suggest not to transmit just one signal but a family of signals. However, even then, in contrary to the univariate case, the density cannot be completely reconstructed. The operator which maps a reflectivity density to its echoes is linear, hence it makes sense to characterize the nullspace of this mapping.

Definition 4.1 *A function $D \in L_2(\mathbf{R}^4)$ is called a* vanishing reflectivity distribution *if the echo* (4.7) *vanishes for any signal $h \in L_2(\mathbf{R}^2)$.*

These vanishing reflectivity distributions can be characterized by their integrals over certain 2D–subspaces. Let $E(\tau, x, \nu)$ denote the 2D–plane defined by

$$E(t, x, \nu) \;=\; \{(\tau_0, s_0, z_0, \sigma_0) \mid \tau_0 = t - \nu s_0,\;\; z_0 = x - \sigma_0 t,\;\; s_0, \sigma_0 \in \mathbf{R}\} \;\; .$$

The nullspace is then characterized by the following lemma.

Lemma 4.2 *A function $D \in L_2(\mathbf{R}^4)$ is a vanishing reflectivity distribution if and only if the integrals of $s_0 D$ over the 2D–planes*

$$\{E(t, x, \nu) \mid t, x, \nu \in \mathbf{R}\}$$

vanish, i.e.

$$0 = \int_{\mathbf{R}} \int_{\mathbf{R}} s_0 D(t - \nu s_0, s_0, x - \sigma_0 t, \sigma_0)\; ds_0 d\sigma_0 \;\; ,$$

for all $(t, x, \nu) \in \mathbf{R}^3$.

Proof:
In order to show that the echoes of a reflectivity distribution vanish for all signals $h \in L^2(I\!R^2)$, it is sufficient that the echoes vanish for all separable signals

$$h(t, x) = h_1(t) h_2(x) \;\; .$$

Inserting this into the model of the echo (4.7) and applying the substitution $\nu = (t - \tau_0)/s_0$ yields

$$\begin{aligned} e(t, x) &= \int_{\mathbf{R}} \int_{\mathbf{R}} \int_{\mathbf{R}} \int_{\mathbf{R}} D(\tau_0, s_0, z_0, \sigma_0) \delta(x - (z_0 + \sigma_0 t))\; h_1\left(\frac{t - \tau_0}{s_0}\right) h_2(z_0 + \sigma_0 \tau)\; d\tau_0 ds_0 d\sigma_0 dz_0 \\ &= h_2(x) \;\; \int_{\mathbf{R}} \int_{\mathbf{R}} \int_{\mathbf{R}} D(\tau_0, s_0, x - \sigma_0 t, \sigma_0)\; h_1\left(\frac{t - \tau_0}{s_0}\right) \;\; d\tau_0 ds_0 d\sigma_0 \\ &= h_2(x) \;\; \int_{\mathbf{R}} \int_{\mathbf{R}} \int_{\mathbf{R}} s_0 D(t - \nu s_0, s_0, x - \sigma_0 t, \sigma_0)\; h_1(\nu) \;\; d\nu ds_0 d\sigma_0 \end{aligned}$$

These integrals have to vanish for any choice of t and x. Moreover, with respect to the variable ν the scalar products with all $h_1 \in L_2(\mathbf{R})$ have to vanish, i.e. a vanishing reflectiviy distribution has to satisfy a.e.

$$0 = \int_{\mathbf{R}} \int_{\mathbf{R}} s_0 D(t - \nu s_0, s_0, x - \sigma_0 t, \sigma_0)\; ds_0 d\sigma_0 \;\; ,$$

which yields the desired charaterization of the nullspace by vanishing integrals of D over 2D–planes. □

Vanishing integrals can only occur if the integrand takes positive and negative values. However, a physically meaningful reflectivity distribution is non–negative, and s_0 lives on the positive part of the real line. Nevertheless two positive reflectivity distributions D_1 and D_2, which only differ by a vanishing reflectivity distribution, cannot be distinguished by any combination of transmitted signals.

The nullspace is characterized by a three-dimensional set of conditions. In order to characterize the complement of the nullspace, i.e., the reconstructable reflectivity distributions, we therefore need to eliminate one of the four variables of $D \in L_2(\mathbf{R}^4)$.

This can be achieved by reducing the dependency of D on σ_0 by fixing the mean velocity as follows: we define

$$\mathcal{D}(\tau_0, s_0, x, t) := \int_{\mathbf{R}} D(\tau_0, s_0, x - \sigma_0 t, \sigma_0) d\sigma_0. \tag{4.9}$$

and assume, that $\mathcal{D}$ can be approximated by its zero order term

$$\mathcal{D}(\tau_0, s_0, x, t) \sim \mathcal{D}(\tau_0, s_0, x, v_0/c), \tag{4.10}$$

compare with (4.4). Furthermore, we have to assume that the family of transmitted signals consists of tensor products

$$h_{m,n}(x, t) := h_m(t) h_n(x), \tag{4.11}$$

where both families $\{h_m\}_{m \in \mathbf{Z}}$ and $\{h_n\}_{n \in \mathbf{Z}}$ form frames in $L_2(\mathbf{R})$.

The first step is to integrate (4.7) with respect to z_0, this yields

$$\begin{aligned} e(\tau, x) &= \int_{\mathbf{R}} \int_{\mathbf{R}} \int_{\mathbf{R}} D(\tau_0, s_0, x - \sigma_0 t, \sigma_0) h_{m,n}\left(\frac{\tau - \tau_0}{s_0}, x\right) d\sigma_0 d\tau_0 ds_0 \\ &= \int_{\mathbf{R}} \int_{\mathbf{R}} \mathcal{D}(\tau_0, s_0, x, t) h_m\left(\frac{\tau - \tau_0}{s_0}\right) h_n(x) d\tau_0 ds_0 \\ &\sim h_n(x) \int_{\mathbf{R}} \int_{\mathbf{R}} \mathcal{D}(\tau_0, s_0, x, v_0/c) h_m\left(\frac{\tau - \tau_0}{s_0}\right) d\tau_0 ds_0. \end{aligned} \tag{4.12}$$

Now the quantity $\mathcal{D}(\tau_0, s_0, x, v_0/c)$ can be reconstructed by using the method explained in Section 2.

5 Numerical Experiments

In this section, we want to demonstrate the applicability of our reconstruction formulae and of the error estimates presented above. The application of our theory to real-life data is still in its elaboration. In particular, 2D–data for signals, which can be modulated arbitrarily in time t and position x, are not available. Nevertheless, to test the algorithm, we proceed as follows: We fix in advance an (artificial) density D in range Doppler coordinates and a suitable frame $\{h_m\}_{m \in \mathbf{Z}}$, compute the corresponding echoes and apply the reconstruction procedure to these echoes. The true density is known in this case, hence, we can estimate and compare the error bounds of different approximation schemes.

First of all, we fix a density D which fits into the setting of our theory: As an manageable example we choose D as

$$D(\tau, s) := e^{i\tau\omega_0} e^{-\tau^2/2} 1_{[-s_1, s_2]}(s) \ ,$$

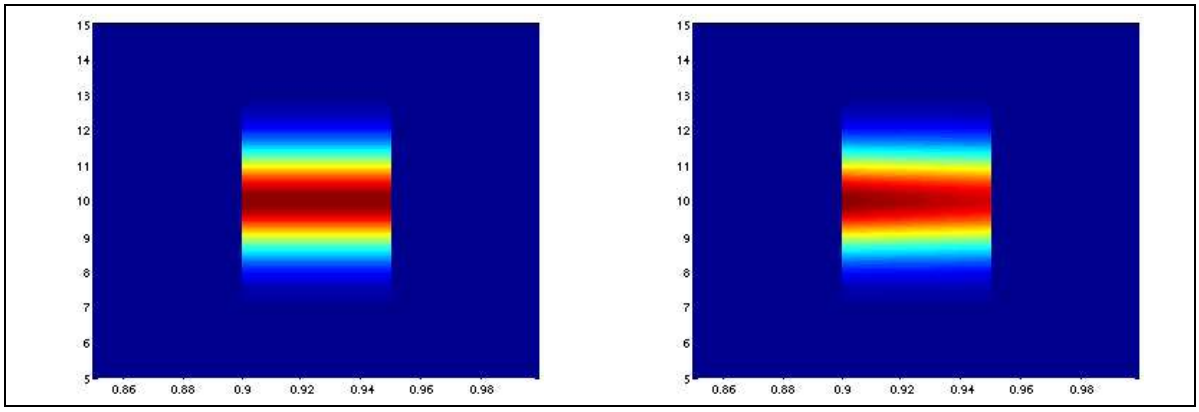

Figure 1: Representation of $\widehat{D(\cdot, s)}(\omega)$ and $\widehat{D(\cdot, s)}(\omega)|s|^{-3/2}$ on the discrete grid $[5.00, 15.00] \times [0.85, 1.00]$.

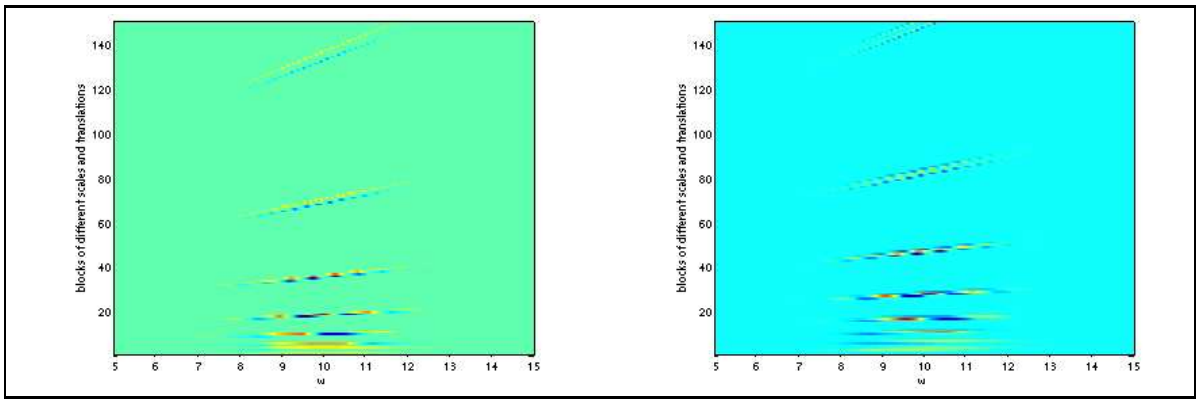

Figure 2: The simulated echoes $\{\hat{f}_m\}_{m\in\mathbf{Z}}$ for the Haar frame (left-hand side) and for the Daubechies-5-frame (right-hand side). The higher scales are not displayed.

where $1_{[-s_1,s_2]}$ represents the characteristic function of the closed interval $[-s_1, s_2]$ and ω_0 describes a shift in Fourier domain. In the sequel, we choose $s_1 = 0.90$ and $s_2 = 0.95$. This reflectivity distribution D satisfies the assumptions of Theorem 2.2.

The outgoing signals have to be a frame. However, since we also want to check the error estimate in Theorem 3.1, a good choice for the frame is

$$h_m(t) = h_{m(j,k)}(t) := \mathcal{F}^{-1}\psi_{j,k}(t) \ ,$$

where $\mathcal{F}^{-1}\psi_{j,k}$ is the inverse Fourier transform of some dilated and translated wavelet, see formula (3.1). In our simulations we used the Haar basis, the Daubechies wavelets of order two, compare [3], and biorthogonal wavelets as constructed in [2], respectively.

Based on the underlying density D we now have to generate families of echoes $\{f_m\}_{m\in\mathbf{Z}}$ which represent the backscattered signals of the transmitted frame $\{h_m\}_{m\in\mathbf{Z}}$. Using the substitution (2.12) we approximate the echoes

$$\hat{f}_m(\omega) = \int_{\mathbf{R}\setminus\{0\}} \widehat{D(\cdot, s)}(\omega)\hat{h}_m(s\omega)|s|^{-3/2}ds$$

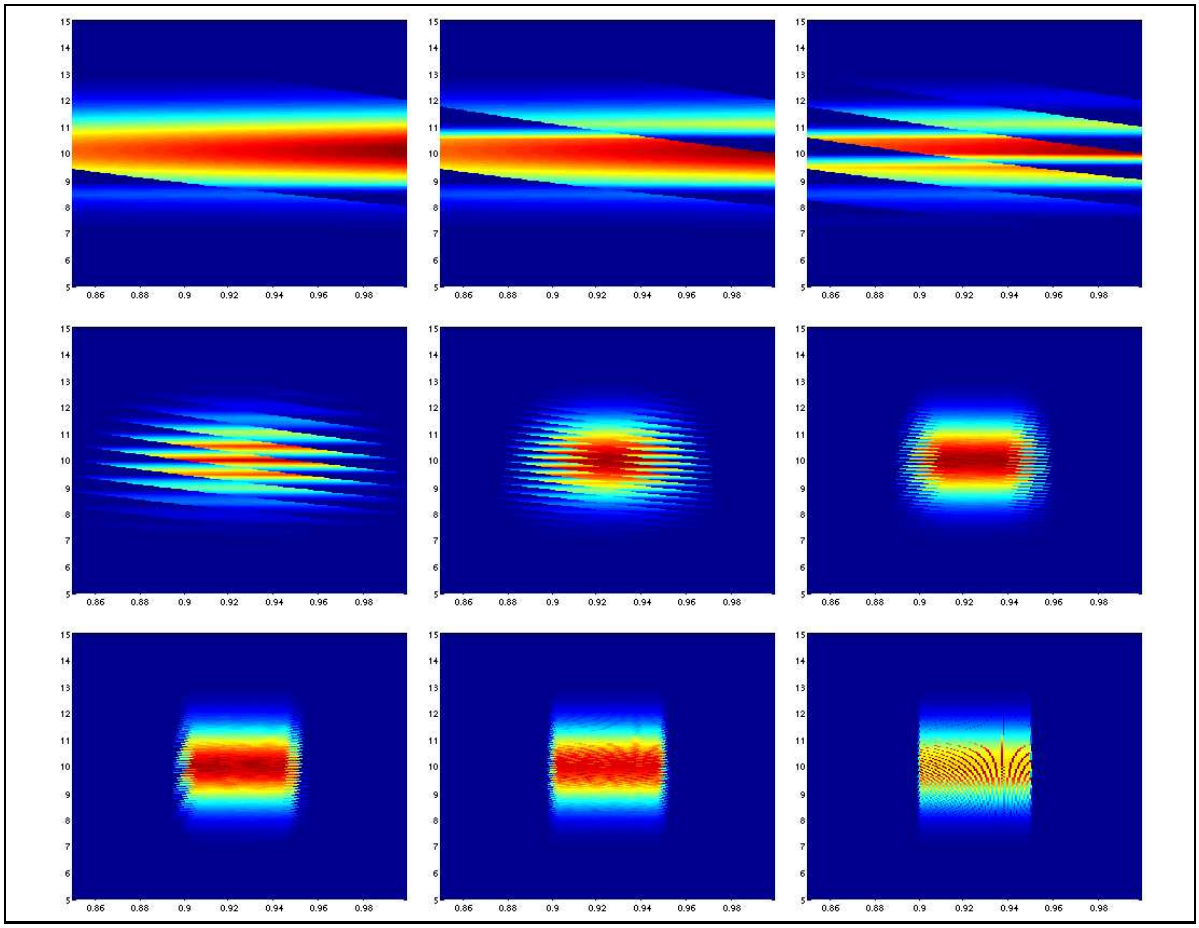

Figure 3: Partial reconstructions based on simulated echoes with respect to the Haar frame. The shown images correspond to the reconstructed densities for $J = -3, -2, -1, 0, 1, 2, 3, 4$ and 6 (from top left to bottom right).

by the corresponding Riemann sums for evaluating these L_2–inner products. A coarse approximation is then given by

$$\begin{aligned} \hat{f}_{j,k}(\omega) &\approx \sum_{s_l \in \Lambda_s} \widehat{D(\cdot, s_l)}(\omega) \psi_{j,k}(\omega s_l) |s_l|^{-3/2} h_l \\ &= \sum_{s_l \in \Lambda_s} e^{-(\omega-\omega_0)^2/2} 1_{[0.90,0.95]}(s_l) 2^{j/2} \psi(2^j \omega s_l - k) |s_l|^{-3/2} h_l \ , \end{aligned} \tag{5.1}$$

where Λ_s describes the grid with respect to the variable s and $h_l = s_l - s_{l-1}$.

Numerically we have to truncate the evaluation of the echoes at some index (j, k). The numerical implementations start at resolution level $j_{\min} = -3$ and end at $j_{\max} = 6$. On the first approximation level $j_{\min} = -3$ we use the echoes produced by translates of the corresponding generator function φ.

For our discretization, we choose $s_l = 0.85 + h_l$, where $h_l = l \cdot 0.00035$ and $l = 0, \ldots, 429$, and $w_r = 5.00 + v_r$, where $v_r = r \cdot 0.025$ and $r = 0, \ldots, 399$. Hence, we have to choose the translation parameter k in such a way that – for all relevant j, r and l –

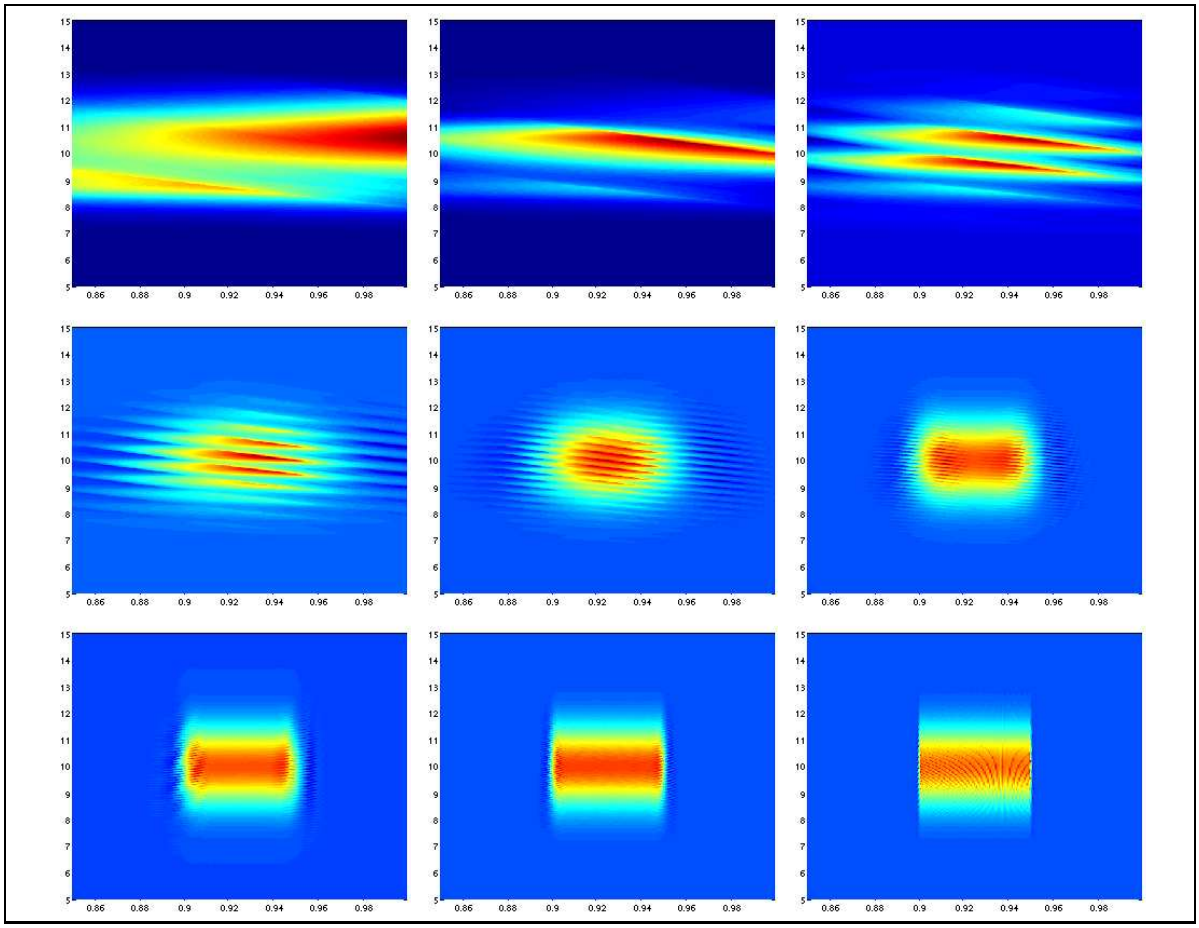

Figure 4: Partial reconstructions based on simulated echoes with respect to the Daubechies frame (N=2). The shown images correspond to the reconstructed densities for $J = -3, -2, -1, 0, 1, 2, 3, 4$ and 6 (from top left to bottom right).

the value of $2^j \omega_r s_l - k$ covers the support of ψ and φ. Figure 1 displays the functions $\widehat{D(\cdot, s)}(\omega)$ and $\widehat{D(\cdot, s)}(\omega)|s|^{-3/2}$ on the rectangle $[5.00, 15.00] \times [0.85, 1.00]$. The resulting echoes approximated by (5.1) are visualized in Figure 2.

Now we are ready to apply the reconstruction formula stated in Theorem 2.2. In order to keep the technical difficulties at a reasonable level, we restrict ourselves to the reconstruction in the Fourier domain:

$$\widehat{D(\cdot, s)}(\omega) = \sum_{m \in \mathbf{Z}} \hat{f}_m(\omega) \widehat{h^m}(\omega s) |\omega| |s|^{3/2} .$$

The quality of the reconstruction is estimated by computing the left hand side of the error estimate of Theorem 3.1. The appraisal has to be taken modulo the integration and scale projection error. The error estimation in Theorem 3.1 was stated in the time domain, Plancherel's Theorem however translates this into an identical estimate in the Fourier domain representation, see (3.8). Additionally, Theorem 3.1 predicts an exponential decay of the error rate, the constants of the estimate depend on the regularity of the

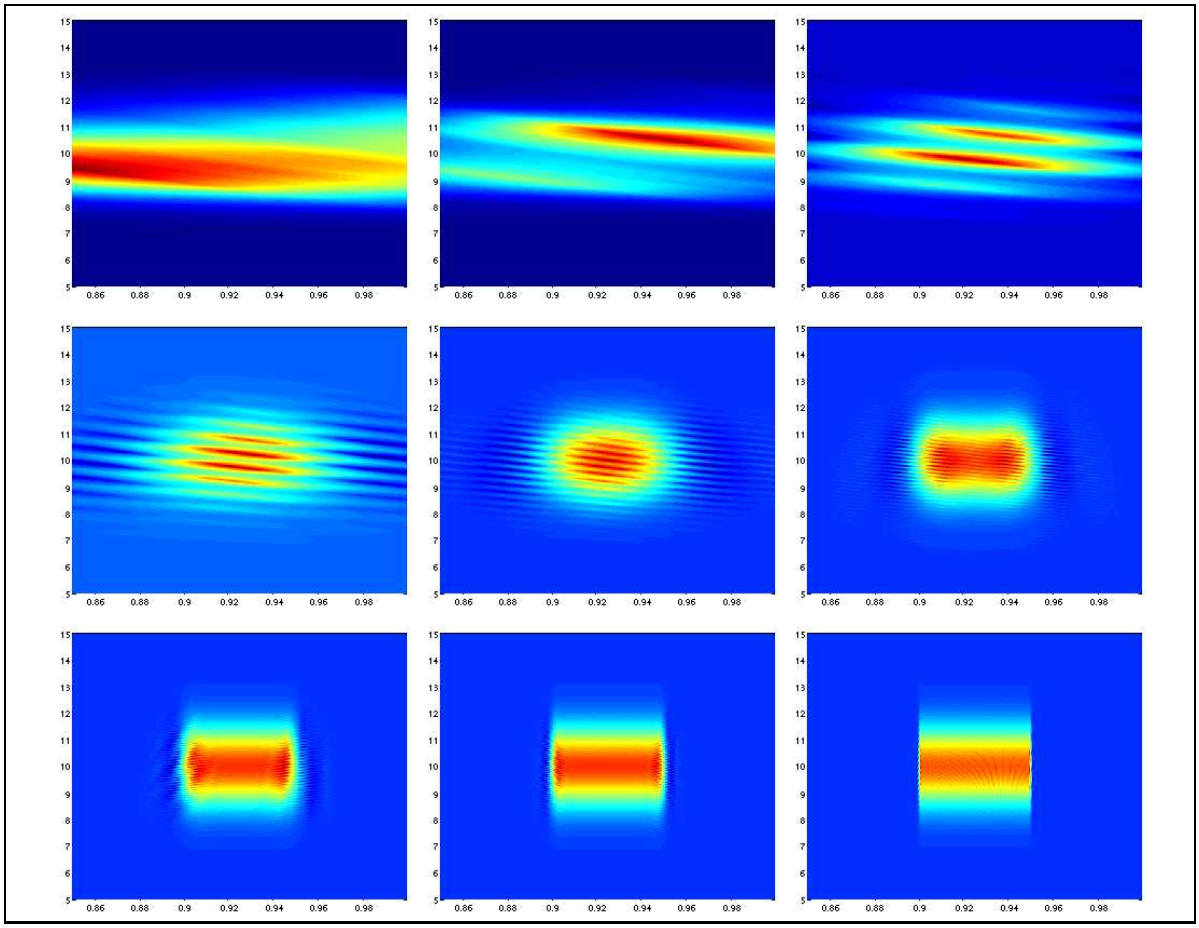

Figure 5: Partial reconstructions based on simulated echoes with respect to the Bior2.4 frame. The shown images correspond to the reconstructed densities for $J = -3, -2, -1, 0, 1, 2, 3, 4$ and 6 (from top left to bottom right).

frame. Indeed, we observe that the weighted L_2–error decreases in the predicted way as the frame regularity increases: We start by presenting a scale-wise reconstruction, see Figures 3, 4, 5 and 6. It turns out that the algorithm converges for all simulated cases. Following Theorem 3.1 we study the error depending on the scale J and on the frame regularity α, respectively. Therefore it is necessary to plot

$$\int_{\mathbf{R}} \int_{\mathbf{R}} \left| \widehat{D(\cdot, s)}(\omega) - \sum_{j \leq J} \hat{f}_m(\omega) \hat{h}_m(s\omega) |\omega| |s|^{3/2} \right|^2 d\omega \frac{ds}{|s|^3} .$$

From Figure 7, left image, we observe that the error indeed decreases exponentially. From the logarithmic plot, right image, we can estimate the parameter α as the slope of the linear least square fit. We deduce the validity of the proposed wavelet based reconstruction algorithm and of the given error estimate.

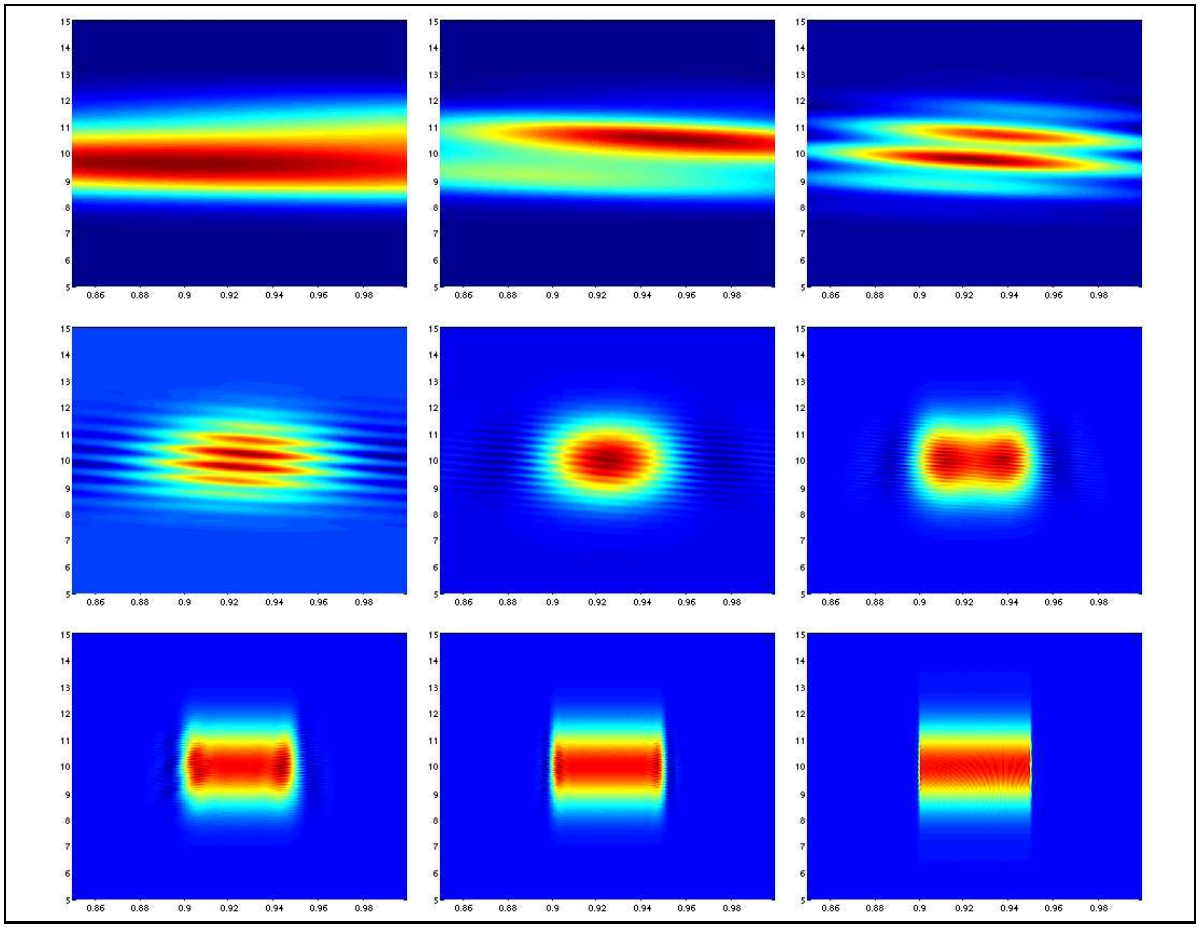

Figure 6: Partial reconstructions based on simulated echoes with respect to the Bior2.8 frame. The shown images correspond to the reconstructed densities for $J = -3, -2, -1, 0, 1, 2, 3, 4$ and 6 (from top left to bottom right).

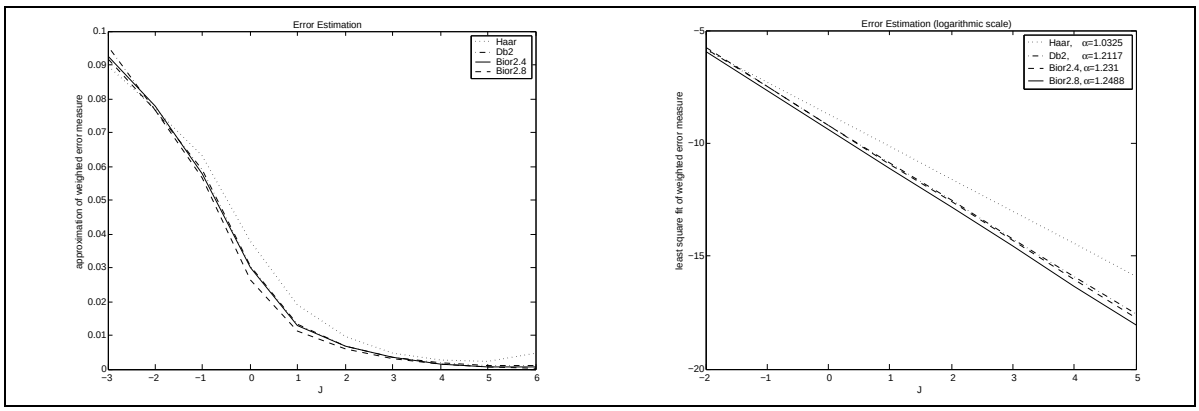

Figure 7: The weighted L_2-error. The left-hand side shows the numerically evaluated error and the right-hand side the linear least square fit in the logarithmic scale.

6 The Narrowband Approach

The wideband model, which describes echoes for arbitrary signals h, can be simplified for most real-life situations. The commonly used narrowband approximation deals with signals of the form

$$h(t) = e^{-i\omega_c t}\eta(t) \ ,$$

where the carrier frequency ω_c is assumed to be much larger then the comparatively narrowbanded frequencies of the modulation function ψ.

Furthermore, most objects of interest in radar travel with a speed much smaller than light. Thus $|v|/c << 1$ and

$$\tau \sim \frac{2R_0}{c}. \tag{6.1}$$

Now we have to treat the positive and negative frequencies of ψ separately

$$\hat{\eta}_P := \hat{\eta}(\omega)\chi_{[0,\infty)}(\omega), \qquad \hat{\eta}_R(\omega) := \hat{\eta}(\omega)\chi_{(-\infty,0]}(\omega). \tag{6.2}$$

Removing the carrier frequency ω_c from both, the signal ψ and the echo f, and neglecting time independent scale factors leads to the standard narrowband model for the echo f of a single moving object

$$f(t) = c\left\{\eta_P(t-\tau)e^{-i\phi t} + \eta_R(t-\tau)e^{+i\phi t}\right\} \ ,$$

where $\phi = 2\omega_c v/c$, see e.g. the classical textbooks [17, 16] and [7] for details. The variables (τ, ϕ) are called the narrowband Doppler coordinates.

Consequently, the narrow–band model for the echo produced by a reflectivity density $D_{NB}(\phi, \tau)$ is given by

$$f(t) = \int_{\mathbf{R}}\int_{\mathbf{R}} \left\{\eta_P(t-\tau)e^{-i\phi t} + \eta_R(t-\tau)e^{+i\phi t}\right\} D_{NB}(\phi,\tau)d\phi d\tau \ . \tag{6.3}$$

We may decompose the space $L_2(\mathbf{R})$ as

$$L_2(\mathbf{R}) \simeq L_{2,P}(\mathbf{R}) \oplus L_{2,R}(\mathbf{R}) \tag{6.4}$$

where

$$L_{2,P}(\mathbf{R}) := \{f \in L_2(\mathbf{R}) \mid \text{supp } \hat{f} \subset [0,\infty), \text{ i.e., } \hat{f}_P = \hat{f}\} \tag{6.5}$$

$$L_{2,R}(\mathbf{R}) := \{f \in L_2(\mathbf{R}), \mid \hat{f}_R = \hat{f}\} \tag{6.6}$$

Then $D_{NB}(\phi, \tau)$ can be reconstructed as follows.

Theorem 6.1 *Let $\{h_m\}_{m\in\mathbf{Z}}, \{g_m\}_{m\in\mathbf{Z}}$ be sets of outgoing signals in $L_{2,P}(\mathbf{R})$ and $L_{2,R}(\mathbf{R})$, respectively. Let us furthermore assume that $\{h_m\}_{m\in\mathbf{Z}}, \{g_m\}_{m\in\mathbf{Z}}$ form frames in these space, and let $\{h^m\}_{m\in\mathbf{Z}}$ and $\{g^m\}_{m\in\mathbf{Z}}$ denote the corresponding dual frames. The echoes*

of $\{h_m\}_{m\in\mathbf{Z}}$ *are denoted by* $f_{P,m}$*, the echoes of* $\{g_m\}_{m\in\mathbf{Z}}$ *are denoted by* $f_{R,m}$*. Let us assume that the reflectivity density* $D_{NB}(\phi,\tau)$ *satisfies the following conditions*

$$h_m(t-\tau)D_{NB}(\phi,\tau)\in L_1(d\phi d\tau),\quad \widehat{D_{NB}(\cdot,\tau)}(\omega)\in L_1(d\omega). \tag{6.7}$$

Then $D_{NB}(\phi,\tau)$ *can be reconstructed as follows*

$$\begin{aligned} D_{NB}(\phi,\tau) &= \frac{1}{2\pi}\sum_{m\in\mathbf{Z}}\int_{\mathbf{R}} f_{P,m}(t)h^m(t-\tau)e^{i\phi t}dt \\ &\quad +\frac{1}{2\pi}\sum_{m\in\mathbf{Z}}\int_{\mathbf{R}} f_{R,m}(-t)g^m(-t-\tau)e^{i\phi t}dt\ . \end{aligned} \tag{6.8}$$

Proof: We proceed by following the lines of the proof of Theorem 2.2. Using (6.3) yields

$$\begin{aligned} f_{P,m}(t) &= \int_{\mathbf{R}}\int_{\mathbf{R}} e^{-i\phi t}h_m(t-\tau)D_{NB}(\phi,\tau)d\phi d\tau \\ &= \int_{\mathbf{R}} h_m(t-\tau)\left(\int_{\mathbf{R}} e^{-i\phi t}D_{NB}(\phi,\tau)d\phi\right)d\tau \\ &= \int_{\mathbf{R}} h_m(t-\tau)\widehat{D_{NB}(\cdot,\tau)}(t)d\tau \\ &= \int_{\mathbf{R}} h_m(\tau)\widehat{D_{NB}(\cdot,t-\tau)}(t)d\tau \\ &= \langle h_m(\cdot),(\widetilde{D_{NB}}(t,\cdot))_P\rangle, \end{aligned}$$

where

$$\widetilde{D_{NB}}(t,\tau) := \widehat{D_{NB}(\cdot,t-\tau)}(t). \tag{6.9}$$

Consequently, by using the reciprocal frame $\{h^m\}_{m\in\mathbf{Z}}$ we obtain

$$\begin{aligned} (\widetilde{D_{NB}}(t,\tau))_P &= \sum_{m\in\mathbf{Z}}\langle(\widetilde{D_{NB}}(t,\cdot))_P,h_m(\cdot)\rangle h^m(\tau) \\ &= \sum_{m\in\mathbf{Z}} f_{P,m}(t)h^m(\tau), \end{aligned}$$

and therefore

$$(\widehat{D_{NB}(\cdot,\tau)}(t))_P = \sum_{m\in\mathbf{Z}} f_{P,m}(t)h^m(t-\tau). \tag{6.10}$$

A similar calculation yields

$$\begin{aligned} (\overline{D}_{NB}(t,\tau))_R &= \sum_{m\in\mathbf{Z}}\langle(\overline{D}_{NB}(t,\cdot))_R,g_m(\cdot)\rangle g^m(\tau) \\ &= \sum_{m\in\mathbf{Z}} f_{R,m}(t)g^m(\tau) \end{aligned}$$

where

$$\overline{D}_{NB}(t,\tau) := \widehat{D_{NB}(\cdot,t-\tau)}(-t). \tag{6.11}$$

Consequently, we obtain

$$(\widehat{D_{NB}(\cdot,\tau)(-t)})_R = \sum_{m\in\mathbf{Z}} f_{R,m}(t) g^m(t-\tau) \tag{6.12}$$

so that

$$(\widehat{D_{NB}(\cdot,\tau)(t)})_R = \sum_{m\in\mathbf{Z}} f_{R,m}(-t) g^m(-t-\tau) \tag{6.13}$$

and

$$\begin{aligned} \widehat{D_{NB}(\cdot,\tau)(t)} &= (\widehat{D_{NB}(\cdot,\tau)(t)})_R + \widehat{D_{NB}(\cdot,\tau)(t)}_P \\ &= \sum_{m\in\mathbf{Z}} f_{P,m}(t) h^m(t-\tau) + \sum_{m\in\mathbf{Z}} f_{R,m}(-t) g^m(-t-\tau). \end{aligned}$$

Again the result follows by applying the inverse Fourier transform

$$\begin{aligned} D_{NB}(\phi,\tau) &= \frac{1}{2\pi}\int_{\mathbf{R}} \widehat{D_{NB}(\cdot,\tau)(t)} e^{i\phi t} dt \\ &= \frac{1}{2\pi}\sum_{m\in\mathbf{Z}} \int_{\mathbf{R}} f_{P,m}(t) h^m(t-\tau) e^{i\phi t} dt + \frac{1}{2\pi}\sum_{m\in\mathbf{Z}} \int_{\mathbf{R}} f_{R,m}(-t) g^m(-t-\tau) e^{i\phi t} dt. \end{aligned}$$

□

References

[1] R.A. Adams, *Sobolev Spaces*, Academic Press, New York, 1975.

[2] A. Cohen, I. Daubechies, and J. Feauveau, Biorthogonal bases of compactly supported wavelets, *Comm. Pure Appl. Math.* **45** (1992), 485–560.

[3] I. Daubechies, *Ten Lectures on Wavelets*, CBMS–NSF Regional Conference Series in Applied Math. **61**, SIAM, Philadelphia, 1992.

[4] R. DeVore, Nonlinear approximation, *Acta Numerica* **7** (1998), 51–150.

[5] R. J. Duffin and A. C. Schaefer, A class of nonharmonic Fourier Series, *Trans. Amer. Math. Soc.* **72** (1952), 341–366.

[6] E. Feig and F.A. Grünbaum, Tomographic methods in range-Doppler radar, *Inverse Problems* **2** (1986), 185–195.

[7] G. Kaiser, *A Friendly Guide to Wavelets*, Birkhäuser, Boston, Basel, Berlin, 1994.

[8] G Kaiser, Physical wavelets and radar – a variational approcah to remote–sensing, *IEEE Antennas and Propagation Magazin* **38** (1996), 15–24.

[9] E. J. Kelly and R.P. Wishner, Matched–filter theory for high–velocity targets, *IEEE Trans. Military Elect.* **9** (1965), 56–59.

[10] A. K. Louis, P. Maass, and A. Rieder, *Wavelets. Theory and Applications*, John Wiley, Chichester, 1997.

[11] P. Maass, Wideband radar: The hyp-transform, *Inverse Problems* **5** (1989), 849–857.

[12] P. Maass, Wideband Approximation and Wavelet Transform, *Proceedings of the IMA* **39**, eds. F.A. Grünbaum et al., Springer, (1990)

[13] H. Naparst, Radar signal choice and processing for dense target environment, PhD thesis, University of California, Berkeley, 1988.

[14] H. Naparst, Dense target signal processing, *IEEE Trans. Information Theory* **37(2)** (1991), 317–327.

[15] L. Rebollo–Neira, A. Plastino, and J. Fernandez–Rubio, Reconstruction of the joint time–delay Doppler–scale reflectivity density in a wide–band regime. A frame theory based appproach, to appear in: *Journal of Mathematical Physics.*

[16] A.W. Rihaczek, *High Resolution Radar*, McGraw–Hill, New York, 1969.

[17] C.H. Wilcox, The synthesis problem for radar ambiguity functions, *Technical Summary Report* **157**, United States Army, University of Wisconsin, 1960.

Berichte aus der Technomathematik ISSN 1435-7968

http://www.math.uni-bremen.de/zetem/berichte.html

— Vertrieb durch den Autor —

Reports **Stand: 30. August 2001**

98–01. Peter Benner, Heike Faßbender:
An Implicitly Restarted Symplectic Lanczos Method for the Symplectic Eigenvalue Problem, Juli 1998.

98–02. Heike Faßbender:
Sliding Window Schemes for Discrete Least-Squares Approximation by Trigonometric Polynomials, Juli 1998.

98–03. Peter Benner, Maribel Castillo, Enrique S. Quintana-Ortí:
Parallel Partial Stabilizing Algorithms for Large Linear Control Systems, Juli 1998.

98–04. Peter Benner:
Computational Methods for Linear–Quadratic Optimization, August 1998.

98–05. Peter Benner, Ralph Byers, Enrique S. Quintana-Ortí, Gregorio Quintana-Ortí:
Solving Algebraic Riccati Equations on Parallel Computers Using Newton's Method with Exact Line Search, August 1998.

98–06. Lars Grüne, Fabian Wirth:
On the rate of convergence of infinite horizon discounted optimal value functions, November 1998.

98–07. Peter Benner, Volker Mehrmann, Hongguo Xu:
A Note on the Numerical Solution of Complex Hamiltonian and Skew-Hamiltonian Eigenvalue Problems, November 1998.

98–08. Eberhard Bänsch, Burkhard Höhn:
Numerical simulation of a silicon floating zone with a free capillary surface, Dezember 1998.

99–01. Heike Faßbender:
The Parameterized SR Algorithm for Symplectic (Butterfly) Matrices, Februar 1999.

99–02. Heike Faßbender:
Error Analysis of the symplectic Lanczos Method for the symplectic Eigenvalue Problem, März 1999.

99–03. Eberhard Bänsch, Alfred Schmidt:
Simulation of dendritic crystal growth with thermal convection, März 1999.

99–04. Eberhard Bänsch:
Finite element discretization of the Navier-Stokes equations with a free capillary surface, März 1999.

99–05. Peter Benner:
Mathematik in der Berufspraxis, Juli 1999.

99–06. Andrew D.B. Paice, Fabian R. Wirth:
Robustness of nonlinear systems and their domains of attraction, August 1999.

99–07. Peter Benner, Enrique S. Quintana-Ortí, Gregorio Quintana-Ortí:
Balanced Truncation Model Reduction of Large-Scale Dense Systems on Parallel Computers, September 1999.

99–08. Ronald Stöver:
Collocation methods for solving linear differential-algebraic boundary value problems, September 1999.

99–09. Huseyin Akcay:
Modelling with Orthonormal Basis Functions, September 1999.

99–10. Heike Faßbender, D. Steven Mackey, Niloufer Mackey:
Hamilton and Jacobi come full circle: Jacobi algorithms for structured Hamiltonian eigenproblems, Oktober 1999.

99–11. Peter Benner, Vincente Hernández, Antonio Pastor:
On the Kleinman Iteration for Nonstabilizable System, Oktober 1999.

99–12. Peter Benner, Heike Faßbender:
A Hybrid Method for the Numerical Solution of Discrete-Time Algebraic Riccati Equations, November 1999.

99–13. Peter Benner, Enrique S. Quintana-Ortí, Gregorio Quintana-Ortí:
Numerical Solution of Schur Stable Linear Matrix Equations on Multicomputers, November 1999.

99–14. Eberhard Bänsch, Karol Mikula:
Adaptivity in 3D Image Processing, Dezember 1999.

00–01. Peter Benner, Volker Mehrmann, Hongguo Xu:
Perturbation Analysis for the Eigenvalue Problem of a Formal Product of Matrices, Januar 2000.

00–02. Ziping Huang:
Finite Element Method for Mixed Problems with Penalty, Januar 2000.

00–03. Gianfrancesco Martinico:
Recursive mesh refinement in 3D, Februar 2000.

00–04. Eberhard Bänsch, Christoph Egbers, Oliver Meincke, Nicoleta Scurtu:
Taylor-Couette System with Asymmetric Boundary Conditions, Februar 2000.

00–05. Peter Benner:
Symplectic Balancing of Hamiltonian Matrices, Februar 2000.

00–06. Fabio Camilli, Lars Grüne, Fabian Wirth:
A regularization of Zubov's equation for robust domains of attraction, März 2000.

00–07. Michael Wolff, Eberhard Bänsch, Michael Böhm, Dominic Davis:
Modellierung der Abkühlung von Stahlbrammen, März 2000.

00–08. Stephan Dahlke, Peter Maaß, Gerd Teschke:
Interpolating Scaling Functions with Duals, April 2000.

00–09. Jochen Behrens, Fabian Wirth:
A globalization procedure for locally stabilizing controllers, Mai 2000.

00–10. Peter Maaß, Gerd Teschke, Werner Willmann, Günter Wollmann:
Detection and Classification of Material Attributes – A Practical Application of Wavelet Analysis, Mai 2000.

00–11. Stefan Boschert, Alfred Schmidt, Kunibert G. Siebert, Eberhard Bänsch, Klaus-Werner Benz, Gerhard Dziuk, Thomas Kaiser:
Simulation of Industrial Crystal Growth by the Vertical Bridgman Method, Mai 2000.

00–12. Volker Lehmann, Gerd Teschke:
Wavelet Based Methods for Improved Wind Profiler Signal Processing, Mai 2000.

00–13. Stephan Dahlke, Peter Maass:
A Note on Interpolating Scaling Functions, August 2000.

00–14. Ronny Ramlau, Rolf Clackdoyle, Frédéric Noo, Girish Bal:
Accurate Attenuation Correction in SPECT Imaging using Optimization of Bilinear Functions and Assuming an Unknown Spatially-Varying Attenuation Distribution, September 2000.

00–15. Peter Kunkel, Ronald Stöver:
Symmetric collocation methods for linear differential-algebraic boundary value problems, September 2000.

00–16. Fabian Wirth:
The generalized spectral radius and extremal norms, Oktober 2000.

00–17. Frank Stenger, Ahmad Reza Naghsh-Nilchi, Jenny Niebsch, Ronny Ramlau:
A unified approach to the approximate solution of PDE, November 2000.

00–18. Peter Benner, Enrique S. Quintana-Ortí, Gregorio Quintana-Ortí:
Parallel algorithms for model reduction of discrete–time systems, Dezember 2000.

00–19. Ronny Ramlau:
A steepest descent algorithm for the global minimization of Tikhonov–Phillips functional, Dezember 2000.

01–01. Efficient methods in hyperthermia treatment planning:
Torsten Köhler, Peter Maass, Peter Wust, Martin Seebass, Januar 2001.

01–02. Parallel Algorithms for LQ Optimal Control of Discrete-Time Periodic Linear Systems:
Peter Benner, Ralph Byers, Rafael Mayo, Enrique S. Quintana-Ortí, Vicente Hernández, Februar 2001.

01–03. Peter Benner, Enrique S. Quintana-Ortí, Gregorio Quintana-Ortí:
Efficient Numerical Algorithms for Balanced Stochastic Truncation, März 2001.

01–04. Peter Benner, Maribel Castillo, Enrique S. Quintana-Ortí:
Partial Stabilization of Large-Scale Discrete-Time Linear Control Systems, März 2001.

01–05. Stephan Dahlke:
Besov Regularity for Edge Singularities in Polyhedral Domains, Mai 2001.

01–06. Fabian Wirth:
A linearization principle for robustness with respect to time-varying perturbations, Mai 2001.

01–07. Stephan Dahlke, Wolfgang Dahmen, Karsten Urban:
Adaptive Wavelet Methods for Saddle Point Problems - Optimal Convergence Rates, Juli 2001.

01–08. Ronny Ramlau:
Morozov's Discrepancy Principle for Tikhonov regularization of nonlinear operators, Juli 2001.

01–09. Michael Wolff:
Einführung des Drucks für die instationären Stokes–Gleichungen mittels der Methode von Kaplan, Juli 2001.

01–10. Stephan Dahlke, Peter Maaß, Gerd Teschke:
Reconstruction of Reflectivity Desities by Wavelet Transforms, August 2001.